

# Exploring seismic data in the flowline domain: Automated extraction of unconformities, facies boundaries and coherent reflections

Dennis Adelled<sup>1,2\*</sup>, Jan Erik Lie<sup>2</sup>, Aina Juell Bugge<sup>2</sup> and Peter Bormann<sup>3</sup>  
The University of Oslo<sup>1</sup>, Aker BP<sup>2</sup>, ConocoPhillips Norge<sup>3</sup>

## SUMMARY

We present a workflow for representing seismic sections as flowlines. The flowlines are extracted as individual objects with a set of properties which makes them easy to work with for various purposes. Here, we focus on (1) extraction of unconformities, (2) identification of seismic sequences and (3) tracking of coherent events. With the proposed workflow, we extract geometric data from the seismic differential dip field. We treat the differential field aligned with seismic reflections as analogous to a fluid velocity field, enabling the tracking of individual flowlines. These flowlines represent the trajectory of imaginary particles carried by the flow, following the fluid's velocity vector at each point. With a scoring system that quantifies overlapping paths, we can identify major unconformity surfaces. Additionally, the flowline representation inherently captures the lateral regional context of a sample, following the seismic geometry. This allows us to group the flowlines into assumed geological packages using available machine learning techniques such as clustering algorithms.

## INTRODUCTION

Seismic reflection data offers detailed subsurface images of the Earth, enabling geologists to delineate geological structures and interpret geological processes, including sedimentation history and tectonic activities. The process of mapping these structures from seismic images demands a substantial investment of time and expertise in seismic interpretation and geophysical comprehension. Each seismic image typically reveals distinct stratigraphic sequences characterized by variations in reflection properties such as continuity, amplitude, and frequency spacing (Badley 1985).

These seismic sequences represent stratigraphic units comprising conformable seismic reflections, indicating intervals of consistent sedimentation conditions influenced by factors like sediment supply and relative sea level. The boundaries of these sequences, defined as unconformities or correlative conformities, mark changes in sediment deposition or non-deposition (Mitchum, Vail, and Sangree 1977). Furthermore, seismic sequences can be categorized into depositional strata packages, such as lowstand, highstand, and transgressive system tracts, providing valuable insights into sedimentary basin evolution (Vail and Mitchum 1977). Understanding these stratigraphic units and their boundaries is fundamental for unravelling the complex evolution of sedimentary basins.

Autotracking tools for seismic interpretation have been readily accessible since the mid-1990s through standard

industry software packages (Eckersley, Lowell, and Szafian 2018; Henderson, Purves, and Leppard 2007; Marroquín 2014; Pauget, Lacaze, and Valding 2009; Veve et al. 2018; Williams 2018). However, despite the availability of autotracking tools, seismic interpretation remains reliant on the manual effort of experienced interpreters. Within the realm of computational and computer-assisted horizon extraction methods, several noteworthy approaches have emerged. These include horizon extraction techniques utilizing unwrapped instantaneous phase volumes (Stark 2003, 2005; Wu and Zhong 2012) and methods based on local reflection slopes (Bakker 2002; Lomask et al. 2006; Wu and Fomel 2018; Wu and Hale 2013). Most existing data-driven methods for horizon extraction successfully track coherent horizons, but they have difficulties to correlate dislocated horizons across faults and along unconformities within structurally and stratigraphically complex seismic volumes. Addressing unconformities resulting from significant erosion poses challenges, especially as they often truncate seismic horizons. Unconformities stand as pivotal features in understanding the evolution of sedimentary basins. Typically, they denote changes in depositional environments due to erosional events or hiatuses. The interpretation of them can be laborious, especially using traditional seismic interpretation methods. Over recent decades, numerous methodologies leveraging computer science, including image processing and machine learning, have been proposed to automate this process (Bahorich and Farmer 1995; Barnes 2000; van Hoek, Gesbert, and Pickens 2010; Wu and Hale 2016).

In this work we present an effective method for representing seismic data as flowlines. The method involves transforming seismic data to the flowline domain by tracking the trajectory of imaginary particles within the differential dip field of the seismic image. This enables us to quickly identify and parameterize the major unconformity surfaces in the seismic image as regions of convergent flowline paths. Our approach is in line with similar methodologies previously introduced, where seismic horizons are delineated by tracking the local dip of seismic events, as demonstrated by Bruin et al. (2006) and van Hoek, Gesbert, and Pickens (2010). However, we distinctly focus on the direct analysis and interpretation of seismic data within the flowline domain itself, rather than primarily deriving secondary attributes, to extract information about the sequence boundaries and the seismic sequences. Furthermore, the flowlines serve as an easy-to-use format for further work, such as with machine learning, for a variety of objectives, including those presented in the work (1) extraction of unconformities, (2)

## Seismic in the flowline domain

identification of seismic sequences and (3) presenting a preliminary workflow for tracking coherent events.

### FLOWLINE METHODOLOGY.

Our method focuses on extracting geometric data from the seismic dip field. To characterize the dip field, we adopt a similar approach to van Hoek, Gesbert, and Pickens (2010) where we estimate the dip field based on the structure tensor. This tensor is defined by its eigenvalues  $\lambda_1 > \lambda_2 > 0$  and the corresponding eigenvectors  $\{e_1, e_2\}$ . The largest eigenvalue,  $\lambda_1$ , and its eigenvector,  $e_1$ , are aligned perpendicularly to seismic reflections, indicating maximum gradient alignment. The smallest eigenvalue,  $\lambda_2$ , with its orthogonal eigenvector  $e_2$ , aligns parallel to seismic reflections, which is central to our analysis. In our study, we treat the differential field aligned with seismic reflections  $e_2$  as analogous to a fluid velocity field. This enables us to track individual flowlines, which are the lines tangent to the velocity vector of the flow at every point. This means that a small imaginary particle moving along the flowline would be carried with the flow, following the direction of the fluid's velocity vector at each point in its path.

Figure 1 illustrates the main steps of the flowline extraction workflow. Figure 1a show the input, a seismic section from the F3 Netherlands block, Figure 1b shows the orientation of the minimum eigenvector  $e_2$  in the seismic section and Figure 1c illustrates the sampling process of the starting position of the flowlines. Figure 1d shows the integrated flowlines for the seismic section sampled on both peak and trough.

### RESULTS

We aim to extract information about the sequence boundaries and the seismic facies from the flowlines. The flowlines serve as an easy-to-use format that can be further utilized in subsequent tasks such as machine learning for various purposes, including those presented in this work (1) extraction of unconformities, (2) clustering seismic facies and (3) tracking coherent events.

We use the Runge-Kutta 4th order (RK4) method, a well-suited numerical solution for ordinary differential equations to integrate the flowlines. The enhanced accuracy of RK4, being a higher-order method, ensures that flowlines are calculated with significantly reduced truncation errors. This allows for a more accurate depiction of the flowlines even when larger step sizes are used, compared to lower-order methods (Butcher 2016). The process for creating the flowlines can be outlined as follows:

- 1) Calculate the structure tensor field from the gradient vector field of the seismic image.
- 2) Define our seismic flow field as the eigenvector  $e_2$  corresponding to the smallest eigenvalue  $\lambda_2$  at each location.
- 3) Initialize the starting coordinate for the flowlines by extracting traces with a fixed increment along the seismic section and picking the time-coordinate on a specific event type on the trace.
- 4) Integrate the flowlines using the RK4 method.
- 5) Store the parametrized path of each flowline for further analysis.

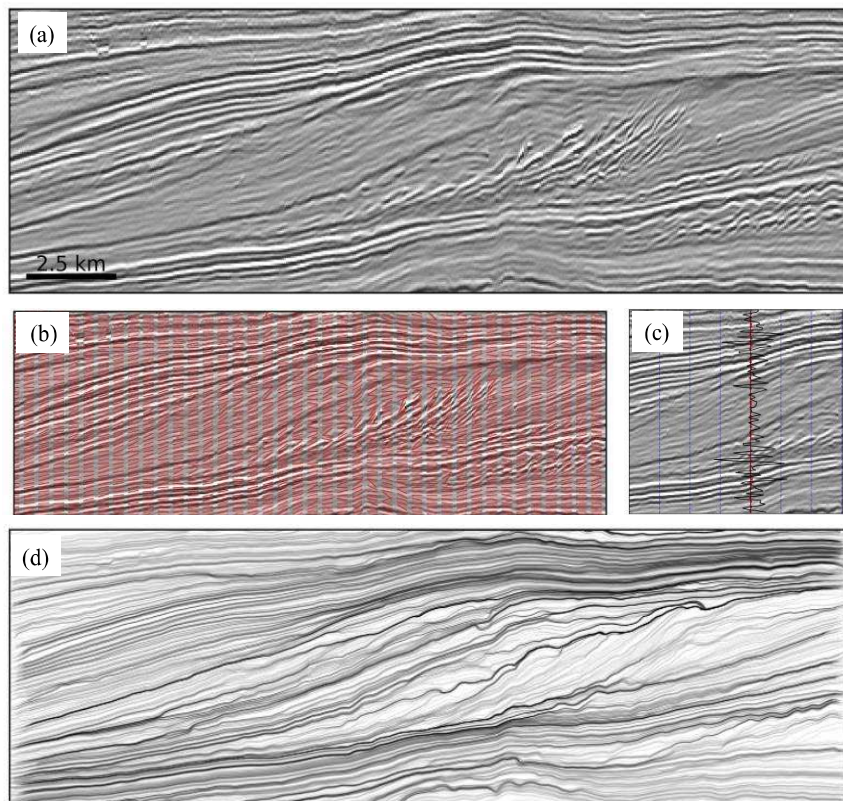


Figure 1: The flowline extraction workflow. (a) Seismic section from the F3 Netherlands block. (b) The orientation of the minimum eigenvectors on the seismic section. (c) The sampling of starting positions for each flowline, picked on events with fixed trace offset increment. (d) The resulting flowlines for the section in (a), picked on both peaks and

## Seismic in the flowline domain

### Flowline unconformity detection.

Each position we initialize a flowline from simulates the path of an imaginary particle placed in our flow velocity field as seen in Figure 1d, where the number of overlapping paths is visualized by the higher opacity in the plot. These surfaces are associated with major unconformities in the system and can partly be explained by their nature of truncating other surfaces, i.e., they share a common path with many surfaces. However, since the major unconformities share a path with all the surfaces that it truncates, both the unconformity surface and the truncated surfaces will obtain a high overlap score. Making it hard to extract the major unconformities on the overlap score alone. In order to extract the major unconformity surfaces, we propose a workflow to remove the truncated surfaces associated with the major unconformities use the following workflow:

- 1) Calculate the overlap score and sort the surfaces in descending order with respect to overlap score.
- 2) We create a list  $S$  to hold our selected surfaces.
- 3) We add a surface  $s_i$  to  $S$  if the overlap between  $s_i$  and any path in  $S$  does not exceed an overlap threshold  $O_{th}$ .
- 4) Continue until all valid surfaces have been added.

The result of the method can be seen in figure Figure 2, where we have plotted the 7 highest scoring surfaces in Figure 2a, which seems to coincide well with some of the major sequence boundaries in the system. The surfaces are numbered based on their overlap score (importance) from highest overlap score (1) to lowest (7). Figure 2b shows 25 highest scoring surfaces superimposed on the seismic section.

### Clustering flowlines to identify seismic sequence

The representation of seismic data through flowlines offers a substantial benefit by more effectively capturing the lateral context of each sample point on a regional scale, based on the seismic geometry. This facilitates the task of grouping flowlines into geological packages using straightforward

clustering techniques. We segment the flowlines into eight distinct clusters, using the distribution of the spatial coordinates of the flowline paths using k-means clustering. Figure 3 shows the delineated seismic section, accurately tracing the major unconformity surfaces evident in the seismic data.

### Tracking coherent events

A further application of the flowline format involves the tracking of coherent events. However, since flowlines are determined based on local dip information, they do not necessarily align with specific event types like peaks or troughs. To address this, we can divide each flowline into smaller segments, with each segment representing only

sequences, obtained by extracting the cluster boundaries from the grouped flowlines. The segmentation aligns well with the presumed stratigraphic sequences within the

one type of event. This segmentation enables the selective analysis of flowlines corresponding to either peaks or troughs. Figure 4 illustrates this concept, showing the tracking of coherent peaks. The peaks are then categorized according to the seismic sequences identified in Figure 3.

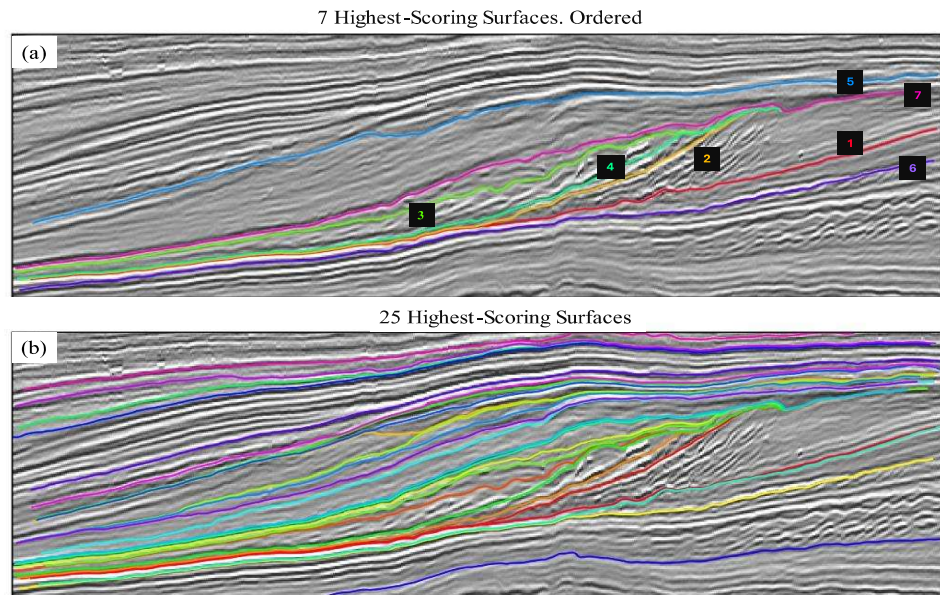


Figure 2: (a) The top 7 highest scoring surfaces with respect to overlap, ordered from highest (1) to lowest (7). (b) The 25 highest scoring surfaces.



## Seismic in the flowline domain

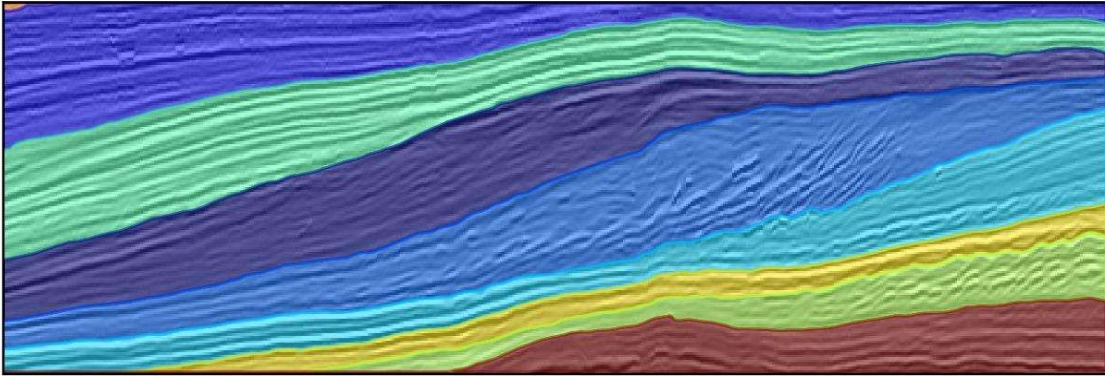


Figure 3: The eight sequences obtained from grouping the flowlines on the x and y coordinates of the flowline paths using k-means clustering.

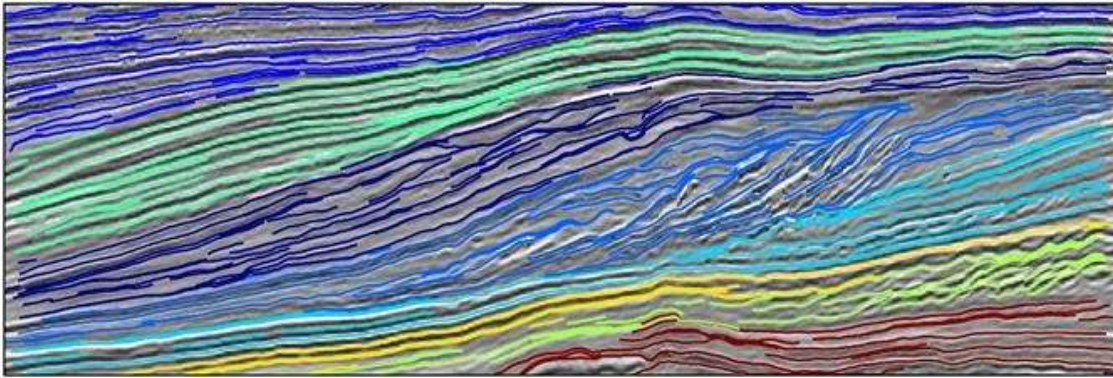


Figure 4: The tracked coherent events, focusing on peak detection. The events are categorized in alignment with our identified seismic sequences.

### CONCLUSIONS

We have developed a workflow that transforms seismic reflection images into a flowline representation, derived from the differential dip field. This method includes a scoring system to evaluate the overlap of flowline paths, allowing for the effective identification and extraction of major unconformity surfaces. Additionally, we show that combining flowlines with seismic amplitude information allows us to track coherent event. Finally, our approach highlights the effectiveness of using the flowline representation of the seismic amplitude image for machine learning applications, such as clustering. This can be attributed to the regional context of each point in

the flowline domain. Our findings suggest that this method has the potential to enhance the efficiency of seismic data analysis, offering a useful tool for advancing geoscientific research and exploration. Furthermore, the flowline format's compatibility with machine learning opens avenues for further exploration and development of more sophisticated workflows.

### ACKNOWLEDGEMENTS

The Netherlands F3 seismic data is provided by dGB Earth Sciences B.V. through OpendTect. D. Adelved would like to thank Aker BP, the Norwegian Research Council and ConocoPhillips Norway for funding and contributing to the ongoing Ph.D. project.